

## PRECUSOR CHEMISTRY FOR THE ACETYLACETONATE-BASED CHEMICAL SOLUTION DEPOSITION OF EPITAXIAL CERIA THIN FILMS

TANIA RISTOIU<sup>a</sup>, LELIA CIONTEA<sup>a</sup>, TRAIAN PETRISOR JR.<sup>a</sup>,  
MIHAI GABOR<sup>a</sup>, TRAIAN PETRISOR<sup>a</sup>

**ABSTRACT.** Cerium acetylacetonate (beta-diketonate)  $\text{Ce}(\text{C}_5\text{H}_7\text{O}_2)_3 \cdot x\text{H}_2\text{O}$  has been used in the preparation of the precursor solution for the deposition of epitaxial ceria thin films. Propionic acid easily dissolves the cerium acetylacetonate resulting in a stable coating solution. The precursor chemistry of the as-prepared coating solution, resulted powder and thin films has been investigated by infrared spectroscopy, mass spectrometry coupled with thermal analysis and X-ray diffraction. The analysis suggests the complex nature of the coating solution due to the formation of a cerium acetylacetonate-propionate mixed ligand complex. The  $\text{CeO}_2$  thin films deposited by spin coating on single crystalline (100) $\text{MgO}$  substrates starting from this solution exhibit a high degree of epitaxy with a  $[h00]||[h00]$  epitaxial relationship between the substrate and the film.

**Keywords:** cerium acetylacetonate, chemical solution deposition (CSD), ceria epitaxial thin films, DTA-TG-MS

## INTRODUCTION

Cerium oxide thin films have a large range of applications in electronics, optics, catalysis, wear resistance, corrosion protection and superconductivity [1]. Pure and doped cerium oxide thin films have been widely investigated as buffer layer for  $\text{YBa}_2\text{Cu}_3\text{O}_{7-x}$  (YBCO) superconducting coated conductors manufacturing. This interest is explained by the smaller lattice mismatch and the similar thermal expansion coefficient of  $\text{CeO}_2$  both with YBCO and the Ni based flexible metallic substrate [2]. Lately, doped ceria is being extensively studied as a potential solid electrolyte for fuel cells [3]. Many deposition techniques have been used for the preparation of  $\text{CeO}_2$  thin films, including both physical [4] and chemical methods [5]. Among the latter, the sol-gel

---

<sup>a</sup> Technical University of Cluj-Napoca, 28, Memorandumului Str., RO-400114, Cluj-Napoca, Romania, [tristoiu@phys.utcluj.ro](mailto:tristoiu@phys.utcluj.ro)

processing route is particularly attractive for the scaling-up of oxide thin films fabrication, since the liquid precursor can easily be applied on a substrate by dipping, spinning or spraying [6,7] and heat treated at lower temperatures.

Metal  $\beta$ -diketonates have become adequate precursors for metal oxides thin films, due to their high volatility, low decomposition temperature, ease of use, commercial availability and relatively low cost. The metal acetylacetonates show a very low solubility in simple alcohols (methanol, ethanol, propanol, butanol) and other organic solvents like toluene, hexane, acetylacetone, but dissolve in propionic acid up to high concentrations. Several attempts have been made to bring into solution the metal acetylacetonates by using carboxylic acids (eg. acetic acid, propionic acid), resulting in a stable coating solution for the deposition of thin films [6].

In this work we report on the fabrication and characterization of cerium oxide thin films on single crystalline (100) MgO substrates starting only from cerium acetylacetonate (2,4-pentadionate) and propionic acid, hereafter denoted in the text by  $\text{Ce}(\text{acac})_3$  and HPr, respectively. Due to the fact that the quality of the thin films strongly depends on the chemistry of the precursor solution, on the thermal treatment, the reactions that take place during the decomposition of the precursor, a special attention has been given to the precursor chemistry.

## RESULTS AND DISCUSSION

### a. Precursor chemistry

#### *FTIR studies*

The FTIR spectra of the precursor solution and the precursor film are given in Figure 1.

From these spectra, information regarding the vibrational modes of the different functional groups present in the precursor have been extracted and compared with the spectra corresponding to pure  $\text{Ce}(\text{acac})_3$  and HPr, as presented in Table 1. The assignment of the most relevant bands is in good agreement with literature data [8-10].

The vibrational modes corresponding to HPr have been identified in the precursor solution, the most significant being located at 1711, 1466, 1236  $\text{cm}^{-1}$  and attributed to C=O stretching,  $\text{CH}_3$  asymmetric bending and C-O stretching, respectively. This is in good agreement with the presence of the HPr excess. It is to be noticed the absence of the vibrational modes corresponding to free propionic acid in the precursor film, as a result of the evaporation of the HPr excess.

New vibrational modes at 1540 (solution) and 1538 (film)  $\text{cm}^{-1}$  are assigned to the  $\nu_{\text{as}}(\text{COO})$  mode in the deprotonated and coordinated propionate ligand. Concomitantly, the  $\nu(\text{C}=\text{O})$  mode of acetylacetonate ligand

found in  $\text{Ce}(\text{acac})_3$  at  $1600\text{ cm}^{-1}$  it is shifted to the above values probably due to a modification of the coordination behaviour.

The coordination of propionate ligand to cerium is also supported by the positiv shift of the  $\nu(\text{C-O})$  mode of HPr ( $1240\text{-}1236\text{ cm}^{-1}$ ) to  $1417\text{ cm}^{-1}$  in the precursor film. According to K. Nakamoto [10], the difference between the two COO frequencies  $\Delta\nu = \nu_a - \nu_s$  is indicative for the coordination of the carboxylate ligand to the metal ion. In our case,  $\Delta\nu = 125\text{ cm}^{-1}$  (precursor solution) and  $\Delta\nu = 128\text{ cm}^{-1}$  (precursor film) lay close to the corresponding value of  $\Delta\nu = 145\text{ cm}^{-1}$  calculated for the sodium propionate. These data suggest a bridging coordination of propionate ligand to the cerium ion.

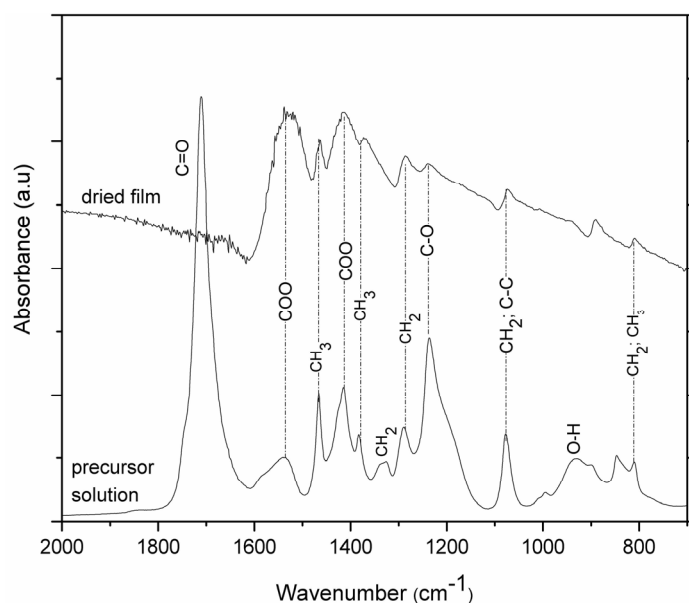


**Figure 1.** FTIR spectra of the precursor solution and dried film.

**Table 1.** Spectral assignment of the main IR peaks

HPr	$\text{Ce}(\text{acac})_3$	Precursor solution	Precursor film	Assignment
1716		1711		$\nu(\text{C=O})$
	1600			$\nu(\text{C}\equiv\text{O})$
		1540	1538	$\nu_{as}(\text{COO}) + \nu(\text{C}\equiv\text{O})$
	1530			$\nu_{as}(\text{C=C})$
1467		1466	1464	$\delta_{as}(\text{CH}_3)$
1416		1415	1417	$\delta(\text{C-O-H}) + \nu_s(\text{COO})$
1384	1395	1383		$\delta_s(\text{CH}_3)$
1325		1326		$\nu_s(\text{CH}_2)$

HPr	Ce(acac) <sub>3</sub>	Precursor solution	Precursor film	Assignment
1291		1289	1286	$\delta_s$ (CH <sub>2</sub> )
	1260			$\nu_s$ C=C
1240		1236		$\nu$ C-O
1080	1020	1078	1074	$\rho$ CH <sub>3</sub> $\nu$ C-C
933		930		$\pi$ O-H
	920			$\nu$ C-CH <sub>3</sub>
848		847		$\nu$ C-C
811		810	810	$\gamma$ CH <sub>2</sub>

### TG-DTA studies

The TG-DTA studies have been performed in dynamic argon atmosphere which actually is poor in oxygen, but not inert, so that the oxidative processes are not completely hindered and the evolved gases can be identified more easily.

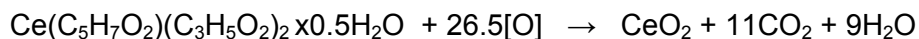
Figure 2 comparatively presents the TG-DTA curves both for cerium acetylacetonate and the precursor powder. The difference between the two curves is clearly seen, suggesting the formation of a new precursor compound. The total weight loss has the value 56.3% for the precursor powder attained around 700°C and sticks to the same value up to 800°C.

The X-ray diffraction pattern of the resulted powder, Figure 3, evidences the presence of CeO<sub>2</sub> only. This enables the calculation of the molecular weight of the estimated precursor of 394 a.m.u., which, in a simplified way, might be attributed to a complex, where two of the acetylacetonate ligands have been replaced by two propionates ligands, Ce(acac)(Pr)<sub>2</sub>x0.5 H<sub>2</sub>O, in agreement with the IR spectra.

From Figure 2 it is observed that all the transformations are associated with a mass loss. This suggests that there is no structural change independent of mass change in the precursor. All the DTA peaks give additional support to the TG results. The precursor is stable up to 80°C. The thermal decomposition of the precursor takes place in three steps:

I. 80 - 275°C, in which the weight loss  $\Delta m = 6.5\%$  is accompanied by an endothermal peak at 232°C.

II. 275 - 500°C, in which the main weight loss takes place,  $\Delta m = 48.9\%$  and, simultaneously, two endothermal peaks at 306°C and 372°C, and one exothermal peak at 430°C. The prominent large exothermal peak is also associated with complex competition oxidation processes, due both to the burning of the organic moieties and to the oxidation of Ce<sup>3+</sup> to Ce<sup>4+</sup>, in agreement with the overall reaction:



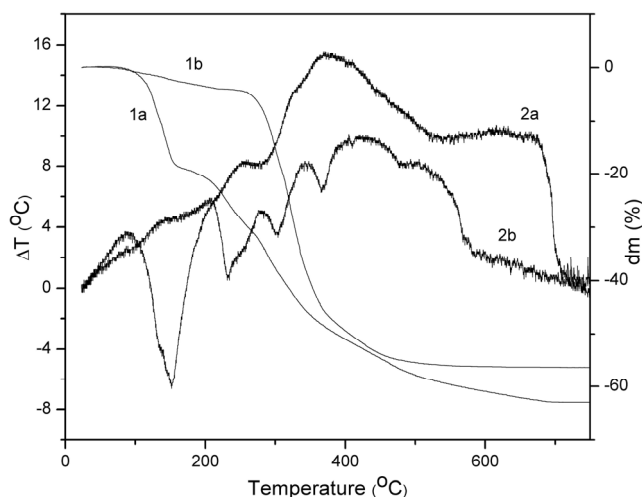


**Figure 2.** TG(1) and DTA(2) analyses for the (a)  $\text{Ce}(\text{acac})_3$  and (b)  $\text{Ce}(\text{acac})_3 + \text{HPr}$

III. 500 - 800°C, in which the weight loss reaches the value of  $\Delta m = 56.3\%$ , the final product being stable from 700°C.

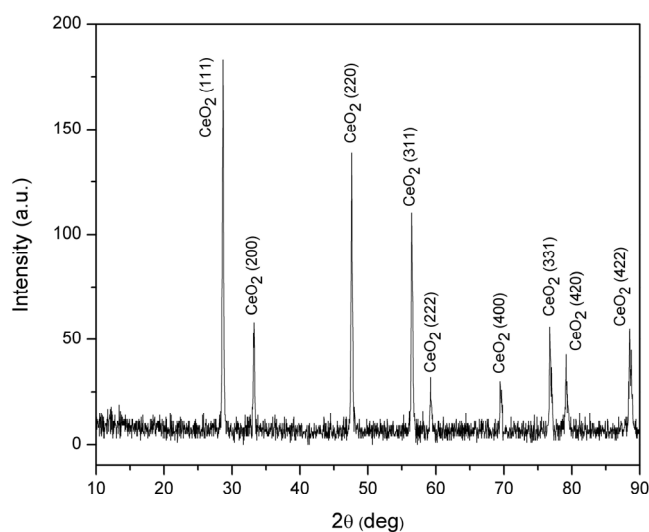


**Figure 3.** X-Ray diffraction pattern of the thermal treated ceria powder

Since the thermogravimetric-differential thermal analyses TG-DTA do not give information about the qualitative aspects of the evolved gases during the thermal decomposition, simultaneous mass spectra of the gaseous reaction products have been performed.

*MS studies*

In Figure 4 three significant mass spectra of the gases evolved during the TG-DTA analyses are presented comparatively. The first spectrum recorded at room temperature (25°C) represents the argon enriched atmosphere,  $m/z = 40$ , for the simple ionized argon atoms and  $m/z = 20$  for the double ionized argon atoms, mentioned above, in which the analyses have been carried out. The mass spectrum registered at 289°C, at the beginning of the second thermal decomposition stage, is characterized by the appearance of the  $m/z = 42$ , 43, 45, 57 peaks, as well as by the significant increase of the  $m/z = 44$ , 22 peaks. At 331°C the greatest number of fragments has been registered in the mass spectrum. Additional broader and more intense peaks appear at  $m/z = 85$ -86, 53-58, 41-46. It is worthwhile mentioning that they are maintained during the entire TG-DTA second stage, but with a smaller intensity.

Due to the fact that the low mass fragments appear in the mass spectra of numerous molecules, it is difficult to attribute them to a certain parent molecular ion. Furthermore, some of the fragments appear at the same  $m/z$  with the background. The heavy fragments registered in the range of the mass spectrometer derive from long chain molecules, some of them might belong to the initial compounds, e.g.  $m/z = 42$ , 85 from  $\text{Ce}(\text{acac})_3$ ,  $m/z=45$ , 57, 55, 56 from HPr, while others can be associated to new molecules, e.g.  $m/z =57$ , 86 from 3-pentanone,  $m/z = 43$ , 86 from 2-pentanone,  $m/z = 43$ , 58, 42 from acetone,  $m/z = 43$ , 85 from acetylacetone or  $m/z = 55$ , 72, 26, 45 from 2-propenoic acid. It is difficult to ascertain their generation, from either the initial ligands or from the complex thermal decomposition products. At the same time, the variety of the  $m/z$  fragments might be attributed to complex attachment mechanism among spatially separated ligands that coordinate the cerium ion as chelating or bidentate bridging, suggested for similar acetylacetonates [9].

In Figure 5 the TG analysis has been superposed onto the temperature dependent evolution of the most frequent fragments in the mass spectra of the precursor at  $m/z = 43$  ( $\text{CH}_3\text{CO}^+$ ), 45 ( $\text{COOH}^+$ ) and, for  $\text{CO}_2$  emission,  $m/z = 44$  ( $\text{COO}^+$ ). The correlation between TG-MS is remarkable, demonstrating a short response time (1s) of the RGA and the accuracy of the method. Nevertheless, the presence of a larger amount of gases prolongues the MS signal even after the end of the emission, leading to a broad band of overlapped effects at 430°C. It is evident that the main weight loss is due to the simultaneous evolution of  $m/z = 43$ , 44, 45 fragments. The significant growth of the  $m/z = 44$  fragment indicates the evolvement of  $\text{CO}_2$  during the combustion of the organic moieties.

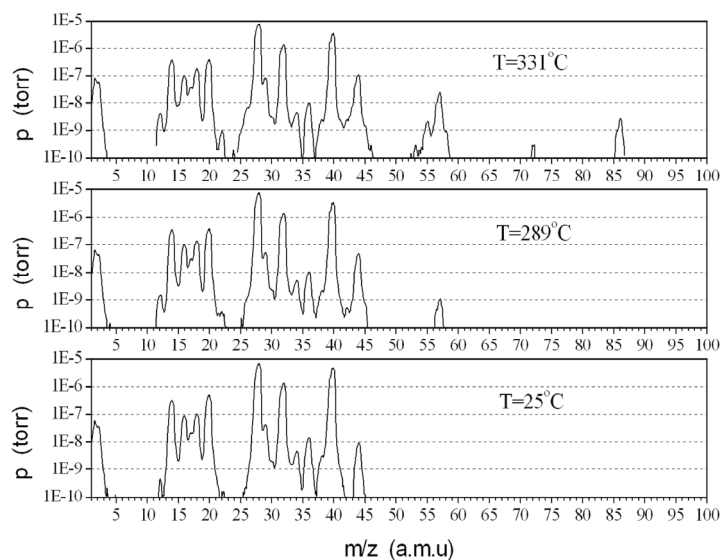


**Figure 4.** The mass spectra of the evolved gasses at different temperatures

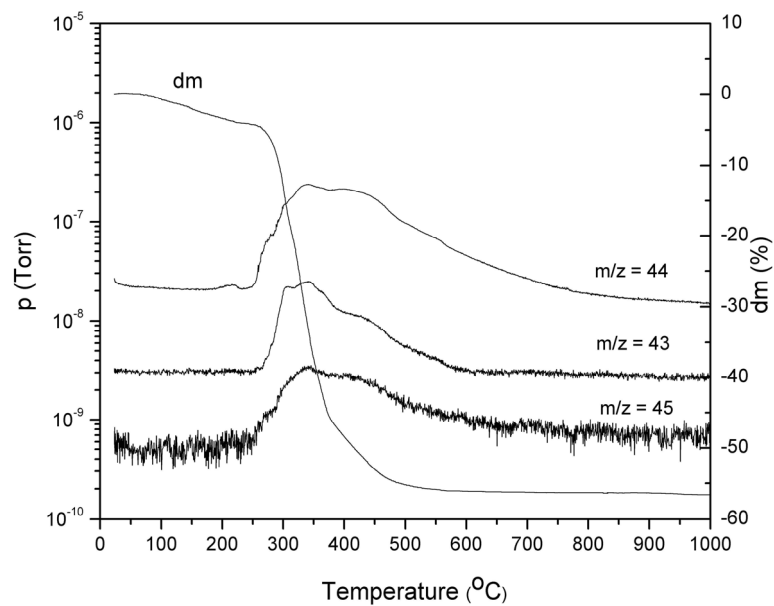


**Figure 5.** Correlated TG-MS analyses for the dried solution

### b. Film analysis

Figure 6 shows the  $\theta$ - $2\theta$  scans for the  $\text{CeO}_2$  films on (100) MgO monocrystalline substrates heat treated at  $1000^\circ\text{C}$  for 15 minutes in  $\text{Ar}+12\%\text{H}_2$  atmosphere and subsequently quenched to room temperature. As it can be seen from the figure, apart for the (200)  $\text{CeO}_2$  peak, no other  $\text{CeO}_2$  reflections are detected. This demonstrates that the  $\text{CeO}_2$  films are epitaxially grown with a  $[h00]||[h00]$  epitaxial relationship between the substrate and the film.

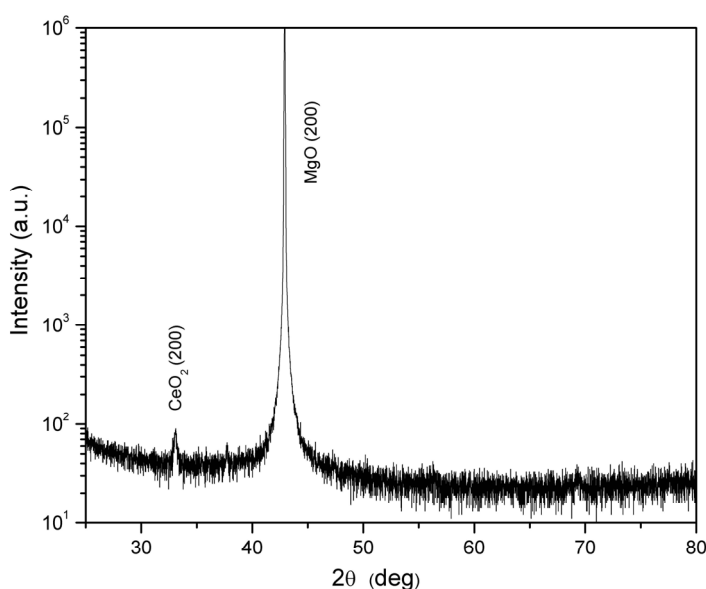


**Figure 6.** The XRD pattern of the (100) MgO/ $\text{CeO}_2$  structures heat treated at  $1000^\circ\text{C}$  for 15 min.

### CONCLUSIONS

Epitaxial 50 nm ceria thin films have been successfully prepared by CSD using only acetylacetonate and propionic acid as reactants, as revealed by X-ray diffraction. Additional informations regarding the thermal decomposition of the precursor coating solution have been obtained from the precursor chemistry studies. By comparing the FTIR spectra and the TG-DTA of the  $\text{Ce}(\text{acac})_3$  and ceria coating solution results that the ceria precursor is most probable a mixed acetylacetonate-propionate complex. This is also sustained by the high  $m/z$  fragments corresponding to the evolvement of 2-, 3-pentanone. In order to understand the chelating process in the coating solution formation

and the complex thermal decomposition processes, higher mass fragments (e.g. cluster) should be considered in the MS analyses. These as obtained epitaxial ceria thin films are promising as buffer layers in the coated conductor architecture and their further structural and morphological characterization is under progress.

## EXPERIMENTAL SECTION

The cerium acetylacetonate,  $\text{Ce}(\text{C}_5\text{H}_7\text{O}_2)_3 \cdot x\text{H}_2\text{O}$  and the propionic acid,  $\text{CH}_3\text{CH}_2\text{COOH}$  with a purity of 99% used in this work were purchased from Alfa Aesar. The coating solution was prepared by mixing 3 mmol of  $\text{Ce}(\text{acac})_3 \cdot x\text{H}_2\text{O}$  in 5 ml of propionic acid (excess) under stirring to form a clear yellow solution. The as-obtained solution was heated at  $75^\circ\text{C}$  resulting in a change of colour to redish-brown. Further, the precursor solution was evaporated to dry powder on an oil bath.

The precursor thin films were deposited by spinning on  $10 \times 10 \text{ mm}^2$  substrates at 4000 rpm for 60 s. Prior to the deposition, the single crystalline (100) MgO substrates were ultrasonically cleaned with isopropanol. The deposition was performed under special cleaning conditions and controlled humidity to hinder the formation of the most common spinning defects (comets and striations) and nonuniform solvent evaporation.

The precursor films were thermally treated in  $\text{Ar}+12\%\text{H}_2$  atmosphere, under different temperature ( $900\text{--}1100^\circ\text{C}$ ) and time (15–45 min.) conditions and quenched to room temperature. Before the heat treatment the samples were purged for about 10 minutes at room temperature in  $\text{Ar}+8\%\text{H}_2$ . The thickness of the films produced under these conditions was typically 50 nm, as resulted from Scherrer equation.

The thermogravimetric-differential thermal analyses (TG-DTA) were performed on the precursor powder, at a rate of  $10^\circ\text{C}/\text{min}$  from ambient temperature to  $900^\circ\text{C}$  in a dynamic atmosphere of argon (20 ml/min), in the temperature range  $20\text{--}900^\circ\text{C}$  using an upgraded computer controlled equipment. The specimens (approximately 0.5 g) were weighed in an  $\alpha\text{-Al}_2\text{O}_3$  crucible.

The TG-DTA has been hyphenated with a quadrupole mass spectrometer QMS 200 atmospheric sampling system, residual gas analyzer (RGA-Stanford Research System) [12, 13], through a 120 cm long stainless steel capillary of an internal diameter of 0.075 mm. The capillary was heated at about  $100^\circ\text{C}$  to prevent the condensation of water and other gaseous products. The acceleration voltage of the ionization was fixed at a potential of 70 eV. Two types of temperature dependent mass spectra were performed, by either registering the selected fragments supposed to be evolved, or the continuous registration between 1–100 a.m.u (in argon dynamic atmosphere).

The precursor was characterized in both solution and film by FT-IR spectroscopy. FT-IR spectra were performed on a Bruker Equinox 55 FT-IR spectrophotometer to identify the IR active functional groups of the precursor molecule. Spectra were collected with  $2\text{ cm}^{-1}$  spectral resolution and 30 scans.

The structural characterization of the thermal analyses resulted powder and of the thin films was performed by X-ray diffraction analysis ( $\theta$ - $2\theta$ ) using a Bruker D8 Discover equipment with Cu K $\alpha$  radiation. The diffractometer is equipped with a graphite monochromator on the diffracted beam to suppress the K $\beta$  component and parasitic scattering.

## ACKNOWLEDGMENTS

The solution preparation was supported by the National University Research Council–Executive Agency for Higher Education and Research Funding (CNCSIS-UEFISCSU), project number PNII-IDEI nr. 4/2010, code 106/2010.

## REFERENCES

1. M.S. Bhuiyan, M. Paranthaman, K.Salama, *Supercond. Sci. Technol.*, **2006**, 19, R1.
2. A. Goyal, R. Feenstra, M. Paranthman, J.R. Thompson, B.Y. Kang, C. Cantoni, D.F. Lee, F.A. List, P.M. Martin, E. Lara-Curzio, C. Stevens, D.M. Kroeger, M. Kowalewski, E.D. Specht, T. Aytug, S. Sathyamurty, R.K. Williams, R.E. Ericson, *Physica C*, **2002**, 382, 251.
3. R. Chockalingam, V.R.W. Amarakoon, H. Giesche, *J. Eur. Ceram. Soc.*, **2008**, 28, 959.
4. V. Boffa, T. Petrisor, S. Ceresara, L. Ciontea, F. Fabbri, P. Scardi, *Physica C*, **1999**, 312, 202.
5. Y. Akin, E. Celik, W. Sigmund, Y. S. Hascicek, *IEEE Trans. Appl. Supercond.*, **2003**, 13, 2563.
6. K. Knoth, B. Schlobach, R. Hunne, L. Schultz, B. Holzapfel, *Physica C*, **2005**, 979, 426–431.
7. L. Ciontea, T. Ristoiu, R.C. Suci, T. Petrişor Jr, T. Petrişor, *AIP Conference Proceeding*, **2007**, 899, 620.
8. H. Provendier, C. Petit, J.L. Schmitt, A. Kiennemann, C. Chaumont, *Journal of Materials Science*, **1999**, 34, 4121.
9. G.B. Deacon, R. J. Phillips, *Coordination Chemistry Reviews*, **1980**, 33, 227.
10. K. Nakamoto, *Infrared and Raman Spectra of Inorganic and Coordination Compounds*, Part B, J.Wiley&Sons, Inc., **2009**.
11. K. Knoth, R. Huehne, S. Oswald, L. Schultz, B. Holzapfel, *Acta Materialia*, **2007**, 55, 517.
12. G.A.M Hussein, H.M. Ismail, *Powder Tech*, **1995**, 84, 185.
13. T. Aii, A. Kishi, M. Ogawa, Y. Sawada, *Anal. Sci.*, **2001**, 17, 875.